Proceedings of the 25th International Conference on
Port and Ocean Engineering under Arctic Conditions
June 9-13, 2019, Delft, The Netherlands

Estimation of static and kinetic friction coefficients for ice interacting with concrete surfaces

Nynke Nuus[1], Stephen E. Bruneau[2], Jeroen S. Hoving[1]
[1] Delft University of Technology, Delft, the Netherlands
[2] Memorial University of Newfoundland, St. John's, Canada

ABSTRACT

Concrete structures in ice prone environments experience abrasion due to ice-structure interaction, where the abrasion is attributed to friction. The sliding friction between concrete and ice is usually described as Coulomb or dry friction and although the physics of dry friction are believed to be well understood, the estimation of the static and kinetic friction coefficients for ice-concrete interaction remains a challenge. Data available in literature is ambiguous and the dependency of friction coefficients on parameters such as normal pressure and velocity is not clear.

To contribute to the existing knowledge about friction coefficients and further investigate the influential factors, ice-concrete friction coefficients were estimated experimentally. With a specially designed set-up, stick-slip tests were performed by placing a cylindrical fresh-water ice sample, connected to a fixed structure by springs on either side, on a rotating slab of low-grade, smooth concrete. During the experiment, normal load (0.7 - 2.0 kg), spring stiffness (80 - 273 N/m) and concrete velocity (0.15 - 0.50 m/s) were varied. Following Coulomb's laws of friction, the static and kinetic friction coefficients were obtained for the given parameters through displacement measurements. In addition, a simplified numerical stick-slip model was developed and validated based on the experimental data.

In this paper, the dependency of the static and kinetic ice-concrete friction coefficients on normal load, spring stiffness and relative velocity is discussed based on test results and a comparison between the experiment and the numerical model is made to further identify the frictional behavior between concrete and ice.

KEY WORDS: Friction; Ice-concrete interaction; Ice abrasion; Stick-slip; Ice model tests;

INTRODUCTION

In the past decades, offshore structures such as piers, bridges, and drilling platforms have been constructed in cold water environments. To deal with ice loading, reinforced concrete is often used as a construction material, because of its great load-withstanding capabilities. However, concrete abrasion due to the continuous sliding interaction with ice is a drawback. Abrasion causes degradation of the concrete surface and can harm the structural integrity when steel reinforcement becomes exposed. Being able to estimate the rate of concrete abrasion due to interaction with ice is crucial for the design process; a correct estimation of the abrasion rate however is a challenge.

Field and lab experiments have been carried out in the past in order to better understand concrete abrasion due to ice. As was concluded by Fiorio et al. (2002), the ice-structure friction conditions play a significant role in the contact behavior. It is generally agreed upon that Coulomb, or dry,

friction is able to describe the frictional behavior between concrete and ice, where a distinction is made between static and kinetic friction forces, that are related to normal load and the static and kinetic friction coefficients, respectively. Several experimental studies have reported on ice-concrete friction coefficients; Table 1 below gives an overview of the coefficients reported by Saeki et al. (1986), Itoh et al. (2002), Fiorio et al. (2002) and Møen et al. (2015).

Table 1. Overview of reported static and kinetic ice-concrete friction coefficients

Author	μ_s (-)	μ_k (-)	v_{rel} (m/s)	P_N (kPa)	T (°C)
Saeki (1986)	0.13 - 0.30	0.050 - 0.250	0.0001 - 10	200	-8
Itoh (1988)	-	0.050 - 0.085	0.05 - 0.2	200	-8
Fiorio (2002)	-	0.260 - 0.360	$1.67 \cdot 10^{-6}$ - $1.67 \cdot 10^{-4}$	25 - 800	-10
Moen (2015)	-	0.039 - 0.054	0.21 - 0.37	500	-10

As shown by Table 1, the reported friction coefficients are ambiguous and the testing parameters have a wide range. Next to that, most authors focus mainly on the kinetic friction coefficient and the distinction between static and kinetic friction is often not addressed. In ISO19906 (2010), the kinetic friction coefficient at velocities ≥ 0.1 m/s is respectively given for rough and smooth concrete as 0.05 or 0.10, while the guidance on the static friction coefficient is limited to stating that it can be 5 times as large as the kinetic friction coefficient at a velocity of 0.1 m/s. This seems a very crude estimation. Furthermore, the variation of the friction coefficients, although given in in ISO19906 by means of a standard deviation, is underrepresented in literature.

In this paper, first the experimental set-up as well as the numerical model are introduced. After which, the test results are analyzed and the obtained friction coefficients are presented along with a discussion of the influence of the design parameters: mass, stiffness and velocity. Then, the experiment is compared with the numerical model, thereby addressing the standard deviation of the friction coefficients and elaborating on the type of friction observed. Finally, a summary of the most important conclusions is given.

EXPERIMENTAL SET-UP

To simulate stick-slip behavior between concrete and ice, a refurbished ice shaper cart with a turntable was used to rotate a concrete slab. A support frame mounted on the side of the cart provided attachment points for the springs that were attached to a cylindrical ice sample. Figure 1a shows the test set-up for the stick-slip experiments and Figure 1b provides a top view and displays the measurements of the set-up.

The concrete slab was made out of medium- to low-grade concrete of the same type as used by Tijsen

Figure 1: Experimental set-up: a) Ice sample support frame next to the octagonal concrete slab on the turntable; b) top view showing the dimensions and degrees of freedom.

(2015). The concrete was poured into an octagonal mold made from formwork plywood and timber, where the concrete exterior facing the formwork was used as the sliding surface, to provide a smooth and regular surface area. The ice sample was made following a procedure similar to the one described by Bruneau et al (2013), using a 100 mm diameter cylindrical plastic mold. After freezing, the ice cylinder was sawn in slices of 50 mm.

In between tests, the rotational velocity of the concrete slab $v_{concrete}$, the spring stiffness k and the normal load on top of the ice sample m, were varied; Table 2 gives an overview of the values used for each of the variables. For each test the displacement of the ice sample were measured in x- and y-direction using a camera in combination with object tracking software. Figure 1b shows how the x- and y-axes are defined.

Table 2. Values for concrete velocity, spring stiffness and normal load used in the tests.

$v_{concrete}$ (m/s)		k (N/m)		m (kg)	
v_1	0.15	k_1	20	m_1	0.67
v_2	0.25	k_2	39	m_2	0.87
v_3	0.37	k_3	50	m_3	1.07
v_4	0.5	k_4	68	m_4	1.12
				m_5	1.32
				m_6	1.58
				m_7	2.03

GOVERNING EQUATIONS FOR STICK-SLIP BEHAVIOR

To interpret and describe the stick-slip behavior as it occurs in the experiments, a simplified numerical model was developed. Figure 2a shows a graphical representation of this model where a 1-mass-spring system, with mass m and stiffness k_m, is placed on a conveyor belt with a drive velocity v_{dr}. It is assumed that the mass is initially placed on the conveyor belt at the equilibrium position such that there is no extension nor compression in the spring. For a non-zero velocity v_{dr}, the mass will initially move along with the belt due to the static friction, so that the relative velocity between mass and belt is zero. This situation is defined as stick mode. The friction force at the surface between the conveyor belt and the mass m_m must then be equal to the force in the spring:

$$F_{fr} = k_m x \tag{1}$$

Here, F_{fr} denotes the friction force and x gives the displacement of the mass m_m relative to the equilibrium position. Equation (1) holds until the critical static friction force is reached, which, assuming Coulomb friction, is related to the normal force F_N and thus the mass m_m as:

$$F_{cr} = \mu_s F_N = \mu_s mg \tag{2}$$

Here, F_{cr} is the critical static friction force, μ_s is the static friction coefficient and g is the standard gravity. The friction force can never be larger than the critical friction force, i.e. $F_{fr} \leq F_{cr}$, so if the force in the spring overcomes the critical friction force, the force at the surface between the conveyor belt and the mass must be balanced by the force due to the acceleration of the mass m_m relative to the motion of the conveyor belt. The corresponding equation of motion reads:

$$m\ddot{x} + k_m x = F_{kin} \tag{3}$$

Here, F_{kin} denotes the kinetic friction force that describes the friction force at the surface between two object moving relative to each other. In correspondence with the critical static friction force, the kinetic friction force is related to the normal force F_N as:

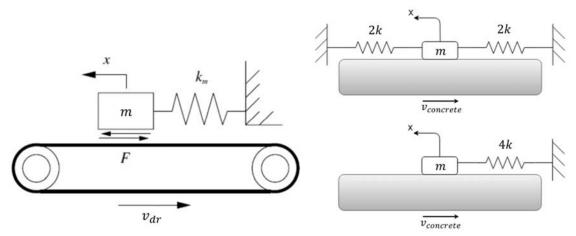$$F_{kin} = \mu_k F_N = \mu_k m_m g \tag{4}$$

Figure 2: a) Graphical representation of a mass-spring system on a conveyer belt; b) side-view of the ice on the concrete slab: springs on both sides versus a spring on one side.

Here, μ_k denotes the kinetic friction coefficient, which is generally has a smaller value than the static friction coefficient. This situation is defined as slip mode. During slip mode, the mass m_m will slide over the conveyor belt until the velocity of the mass again becomes equal to the drive velocity v_{dr}, after which it will transition back to stick mode. The process of alternating between stick and slip-mode will repeat itself as long as the belt keeps running.

To identify the static and kinetic friction coefficients that occur during the experiments, we assume that the interaction between the ice sample and the rotating concrete slab may be well described by Coulomb's law and may therefore be described by equations (1) to (4). Note here that, when using equations (1) to (4) to describe the experiments, the stiffness k_m must be replaced by a stiffness $4k$ to represent the 4 springs in the experimental set-up in accordance with the two equivalent representations of the experiments given in Figure 2b. To determine the static and kinetic friction coefficients μ_s and μ_k from the displacement measurements using equations (1) to (4) however, we must first identify the stick- and slip-modes from the measurement data.

EXPERIMENTAL DATA ANALYSIS

As stated above, the measurement data consists of the displacements of the ice sample in x- and y-direction as obtained by using object tracking software on visual camera recordings. As the displacements in y-direction appeared to be negligible compared to the displacement in x-direction, only the displacement in x-direction are used here. The velocity and acceleration of the ice sample in x-direction are derived from the displacements in x-direction numerically.

In the following, we will first elaborate on the identification of the stick- and slip-modes, after which we will respectively determine and discuss the resulting static and kinetic friction coefficients, including their dependencies on the test variables $v_{concrete}$, k and m.

Identification of stick- and slip-modes

Figure 4a shows the velocity of the ice sample, given by the blue line, as a function of time as derived from the test data for a typical data set in comparison with the local velocity of the concrete, given by the green line. Additionally, the red circles denote data points at which the system is in stick-mode, while at the remaining data points the system is in slip-mode. Here, the stick- and slip- modes are identified from the test data using the following definitions:
- During stick, the ice velocity is equal to the local concrete velocity: $v_{ice} = v_{concrete}$.
- During slip, the ice velocity is not equal to the local concrete velocity: $v_{ice} \neq v_{concrete}$.

Additionally in Figure 4b, the velocity of the ice sample in the proximity of the local concrete velocity is magnified for the time period between 9 and 12 seconds.
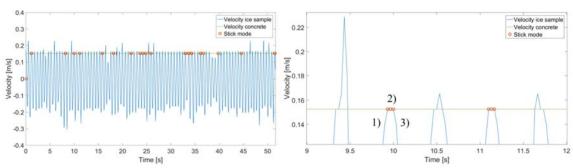
Figure 4: a) Velocity of the ice sample as a function of time; b) Velocity of
the ice sample in the proximity of the local concrete velocity;

In general, the velocity of the ice sample during slip may be expected to be smaller than the velocity of the concrete at that location. The reason for this is that when the cumulative force in the springs overcomes the static friction force, the net force is opposite to the direction of motion, causing the ice sample to slow down. The test data presented in Figure 3 however suggests otherwise. In Figure 4b, the second and fourth peak clearly show the occurrence of stick in accordance with the definition given above. For both peaks, the behavior can be described by the following stages as numbered for the second peak in Figure 4b:

1) While the ice sample is in slip mode, its velocity increases until the ice sample velocity reaches the local concrete velocity and the system transits from slip- to stick-mode.
2) While the system is in stick-mode, the ice sample velocity is equal to the local concrete velocity until the critical static friction force is overcome by the forces in the springs and the system transits from stick- to slip-mode.
3) As the ice sample transits back into slip-mode, the net force on the ice sample works opposite to the direction of motion, causing the ice sample to slow down.

The three other peaks in Figure 4b however, do not show the behavior that is to be expected based on the given definitions. Whereas one of the data points in the first peak gives an ice sample velocity of approximately 0,23 m/s that extends far beyond $v_{concrete}$, the other data points in the first, third and fifth peak that extend beyond $v_{concrete}$ all have a velocity that is exactly 0.013 m/s higher than the local concrete velocity . The occurrence of these velocities higher than the local concrete velocities may be explained either by:

▪ measurement errors or errors in measurement technique, or by
▪ two-dimensional behavior of the ice sample.

Measurement errors or errors in measurement technique
Due to the motion in the test setup, i.e. the rotation of the concrete slab and the motion of the ice sample, vibrations may have occurred in the test set-up that may have translated into motion of the camera. Consequently, this may have caused some random errors in the displacement measurements. Furthermore, it was noticed that the camera was slightly sensitive to the lightning conditions; shadows over the red square on the ice sample caused the camera not to pick up on the full colored square, which was the recognition point for the object tracking software. Lastly, the sampling frequency of

Figure 3: Top view of the ice sample: a) without rotation; b) with rotation.

30 frames per second recorded by the camera may have compromised the detection of stick and slip cycles at high stick-slip frequencies, although this is not valid for the data shown in Figure 4.

Two-dimensional behavior of the ice sample
Whereas the definitions of the stick- and slip-modes are based on the one-dimensional motion of the mass m as depicted in Figure 2a, the experimental test set-up allows for two-dimensional motion of the ice sample. Next to the displacement in x-direction, the ice sample can move in y-direction, as well as rotate around its center of gravity. As previously stated, the y-displacement is negligible and therefore its influence on the stick-slip behavior is as well. During the tests, the ice sample significantly rotates around its own center of gravity as is shown by Figure 3. The rotation of the ice sample is induced by the rotation of the concrete slab, which causes the velocity of the concrete to have a gradient over the width of the ice sample during slip. This in itself naturally introduces some rotation in the ice sample. Additional rotation of the ice sample may be explained by the variation of surface roughness over the concrete slab. Figure 3 shows that, due to the location of the red square on the ice sample, its rotation causes the red square to move differently than the center of the ice sample.

Generally, the ice sample rotates back to its equilibrium position (Figure 3a) during transitions between the stick- and slip-modes. This may explain the occurrence of velocities higher than $v_{concrete}$ during the stick-mode. In fact, based on the geometry, an estimation can be made of the increase in velocity experienced by the red square compared to the velocity of the center of the ice sample. This estimation shows that the difference in velocity experienced by the red square in comparison with the center of the ice sample is in the order of 0.013 m/s and therefore has the same order of magnitude as the small peaks in Figure 4b, so that the velocity of the center of the ice sample during these peaks was, in fact, equal to the velocity of the concrete at that location. Visual confirmation shows that rotation of the ice sample occurred during the first, third and fifth peak in Figure 4b. Based on this, we conclude that the rotation of the ice sample explains that even though the system was in stick mode, the measured displacements yields the small velocity peaks observed in the data.

This however does not explain the large velocity in the first peak in Figure 4b, which is therefore contributed to measurement errors. Due to the difficulty of straightforwardly detecting the stick-mode in situations where the ice sample velocity is larger than the local concrete velocity, these data points have been excluded from the data used to determine the static and kinetic friction coefficients.

Determining the static friction coefficient

From Coulomb's law of friction it follows that, at the moment of stick-to-slip transition, the friction force at the surface between the concrete slab and the ice sample, given by equation (1) by substituting $k_m = 4k$, must be equal to the critical static friction force, as described by equation (2). Rearranging the resulting equality, the static friction coefficient can straightforwardly be derived from the displacement of the ice sample at the moment of stick-to-slip transition as:

$$\mu_s = \frac{4kx_{stick}}{mg} \tag{5}$$

Here, x_{stick} is the displacement of the ice sample at the moment that stick occurs. Based on applying equation (5), it was observed that over the course of a single test there is a variation of the static friction coefficient over time. Figure 5 and **Error! Reference source not found.** therefore present the dependency of the static friction coefficient on the test variables $v_{concrete}$, k and m in the form of its mean and its standard deviation.

The downward trend in the graphs for the mean static friction coefficients in Figure 5 and **Error! Reference source not found.** indicate that an increase in mass, and thus an increase in normal force, yields a decrease of the mean static friction coefficient. Additionally, by comparing the results for the velocities v_1 to v_4, we find that an increase in local concrete velocity slightly decreases the mean static friction coefficient.

In literature, no references to the influence of normal load on the static friction coefficient for ice-concrete interaction were found. For steel-ice interaction however, Terashima and Nakazawa (1993) show that an increase in normal load causes a decrease in static friction coefficient, upon approaching a constant above a normal stress of 0.5 MPa. According to Terashima and Nakazawa, an increase in normal stress on the surface causes the asperities to break off and smooth the surface, therefore decreasing the static friction coefficient. The occurrence of a similar effect in ice-structure interaction can explain the result that are observed here. A decrease of the static friction coefficient caused by an increase in sliding velocity was also observed by Saeki et al. (1986). Saeki et al. attribute this to the fact that the actual contact area diminishes at higher velocities, where the surfaces start riding over each other. This is also in line with the effect of static strengthening as discussed by Schulson and Fortt (2013): a higher velocity means less time for the asperities to lock into each other and thereby lowering the friction coefficients.

Figure 5 and **Error! Reference source not found.** additionally show that for the spring stiffnesses k_1 to k_3, an increase in spring stiffness causes an increase in the mean static friction coefficient. For
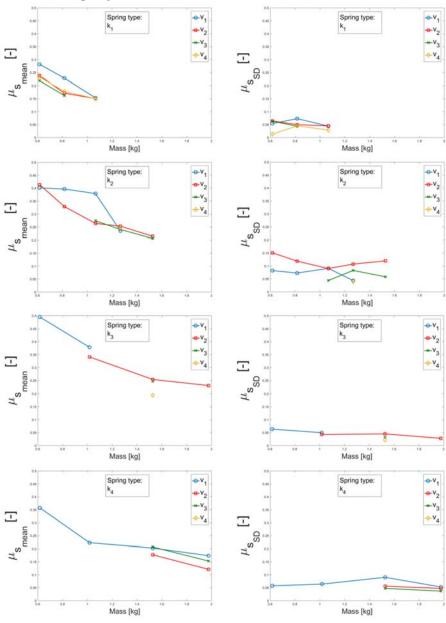

Figure 5: Static friction coefficient as a function of applied mass for velocities v_1 to v_4:
a) mean for k_1; b) standard deviation for k_1; c) mean for k_2; d) standard deviation for k_2;
e) mean for k_3; f) standard deviation for k_3; g) mean for k_4; h) standard deviation for k_4;

the spring stiffness k_4 however, this trend does not continue. The influence of the spring stiffness on the static friction coefficient is therefore not clearly identified. The standard deviation of the static friction coefficient is smaller than the mean, however a clear dependency of the static friction coefficient on velocity, spring stiffness or mass is not observed.

Determining the kinetic friction coefficient

During slip mode, the interaction between the ice sample and the concrete slab is described by equation (3), where $k_m = 4k$. Here, the friction force at the surface between the concrete slab and the ice sample is equal to the kinetic friction force as described by equation (4). Substituting equation (4) into equation (3) and rearranging yields the kinetic friction coefficient as:

$$\mu_k = \frac{m\ddot{x}_{slip} + 4kx_{slip}}{mg}\mu_k = \frac{m\ddot{x}_{slip} + 4kx_{slip}}{mg} \tag{6}$$

Here, x_{slip} and $\ddot{x}_{slip}$ are respectively the measured displacement and numerically derived acceleration of the ice sample during slip. Similar to the static friction coefficient, the tests show that the kinetic friction coefficient as determined by using equation (6) continuous varies over time. Therefore, Figure 6 and Figure 7 present the mean and the standard deviation of the kinetic friction coefficient as they depend on the test variables $v_{concrete}$, k and m.

The mean of the kinetic friction coefficient in Figure 6 and Figure 7 shows a decreasing trend with increasing normal load. This corresponds to findings in literature by Fiorio et al. (2002) and Møen et al. (2015). When considering the different velocities v_1 to v_4, we observe that a velocity increase yields a decreasing kinetic friction coefficient. This is consistent with previous findings by Martins et al. (1990), Møen et al. (2015) and Saeki et al. (1986). According to Saeki et al., an increase in velocity gives less opportunity for the asperities of both surfaces to lock into each other and thereby reduces the actual contact area while the surfaces slide over each other. Møen et al. additionally note that a higher velocity yields an increase of frictional heating causing a thin water layer to lubricate the ice-concrete interface.
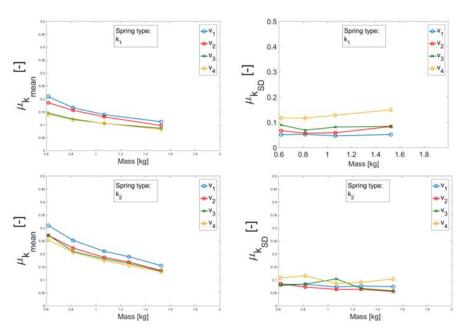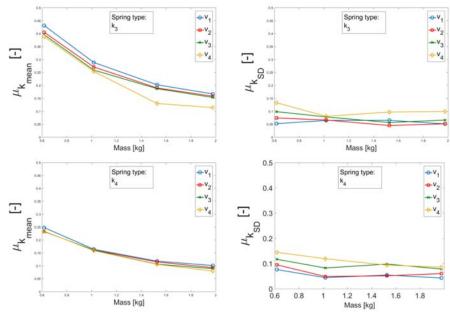

Figure 6: Kinetic friction coefficient as a function of applied mass for velocities v_1 to v_4: a) mean for k_1; b) standard deviation for k_1; c) mean for k_2; d) standard deviation for k_2;

Figure 7: Kinetic friction coefficient as a function of applied mass for velocities v_1 to v_4: a) mean for k_3; b) standard deviation for k_3; c) mean for k_4; d) standard deviation for k_4;

In correspondence with the static friction coefficients, Figure 6 and Figure 7 show that an overall increase in spring stiffness yields an increase of the kinetic friction coefficient for k_1 to k_3. Spring stiffness k_4 however does not follow this trend. The fact that this trend persists for both the static and the kinetic friction coefficient, and for several test runs, indicates that the lower coefficient is not due to an error measurement or different ambient conditions. The most likely explanation is that for a larger spring stiffness, and thus for larger friction forces, the way the ice and the concrete interact changes. For example, at low friction forces the asperities of both the ice and concrete surface may remain intact yielding a relatively high friction coefficient, while at high friction forces the asperities may break off yielding a lower friction coefficient. This effect may also be related to ductile versus brittle failure of the asperities at different friction forces, but this has not been further explored in this paper.

The standard deviations of the kinetic friction coefficient are larger than those observed for the static friction coefficient. Especially for the smallest spring stiffness and for the largest concrete velocity, i.e. for k_1 and v_4, the order of magnitude of the standard deviation is similar to that of the mean value. In fact, from Figure 6 and Figure 7, it appears that a higher velocity yields a larger variation of the kinetic friction coefficient. For the variation in spring stiffness and mass however, no clear trends are identified.

Comparing the results for the static and kinetic friction coefficients, it is clear that the trends for the kinetic friction coefficient are smoother and therefore more pronounced. This is due to the much larger set of data points available during slip mode. The mean ratio between the kinetic and static friction coefficients compared per test run is found to be 0.7.

VALIDATION OF A SIMPLIFIED MODEL BASED ON THE TEST RESULTS

As stated previously, Figure 2a is a graphical representation of a simplified numerical model that is able to describe the stick-slip behavior between the ice sample and the concrete slab. One of the constraints of this numerical model is that it considers the stick-slip interaction in one-dimension. As previously discussed, during the experiments the ice sample showed certain two-dimensional behavior that influenced the test results. Although this two-dimensional behavior of the ice sample cannot be incorporated into the simplified numerical model, there are several aspects of the frictional ice-concrete interaction observed in the tests that can be incorporated in the simplified model. In the following, the implementation of these aspects into the simplified model are addressed and validated

based on the test data in order to reflect on the assumptions made with respect to the experimental data.

Randomness and time dependence of the friction coefficients
To mimic the experiments, the friction coefficients that are obtained from the experiments have been used as input in the numerical model. This can be done by using the mean value of the friction coefficients, but this does not yield an accurate representation of the irregular coefficients observed during the experiment. In the numerical model therefore, at every transition to stick- or slip-mode, the corresponding static and kinetic friction coefficients were obtained from a Gaussian distribution defined by the mean and standard deviations for the friction coefficients obtained from the experiments. Incorporating this into the model, results in displacements and velocities that are similar to those measured during the experiments. The sensitivity of the numerical model to changes in input was tested and it was verified that the model works appropriately, i.e. the change in output due to a change in input is similar to what is observed in the experimental data.

It should be noted here that, in the numerical model, the value of the kinetic friction coefficients has been regulated in such a manner that, although its normally distributed, the kinetic friction coefficient may never have a larger value than the preceding static kinetic friction coefficient, as this would results in ice sample velocities larger than the local concrete velocities. Additionally, in the model, both the static and kinetic friction coefficients are constants during each instance of respectively stick and slip that only change when the next mode transition occurs.

The resulting variation of the kinetic friction coefficient over time is depicted for the numerical model in Figure 8b, while Figure 8a depicts the kinetic friction coefficient over time as it is obtained from a test run with corresponding variables. Comparing the dependency of the kinetic friction coefficient over time in respectively the tests and the model, it is clear that during the experiments the kinetic friction coefficient is not a constant during each period of slip, even though it is implemented as such in the numerical model. This dependency over time during each period of slip can partly be explained by spatial variation of the surface roughness of the concrete slab. This variation in surface roughness however does not sufficiently explain the rather large and chaotic variation of the kinetic friction coefficient over time during a single slip-period. Next to the variation during each period of slip, Figure 8a additionally shows a global periodicity of the kinetic friction coefficient over time, which can be attributed to the location of the ice sample on the concrete slab. Due to its circular path, skewing of the slab or a pattern in surface roughness over the slab leads to a repetitive pattern in the kinetic friction coefficient over time. Note here however that this periodic effect could not be observed in the displacements measured during the tests.

Neither the time dependency of the kinetic friction coefficient during each period of slip, nor the global effect attributed to the rotation of the slab, are accounted for in the numerical model. This is not only because the phenomena were not well understood, but also because implementing these dependencies statistically did not yield an improvement in performance of the numerical model. Despite this, Figure 8 shows that the kinetic friction coefficient in the tests and in the model roughly have the same range. The statistical similarity between model and tests are further discussed below.
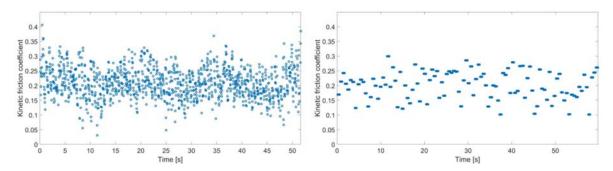

Figure 8: Kinetic friction coefficient over time: a) in the tests; b) in the model.

Influence of the memory effect on the friction coefficients

When using the friction laws of Coulomb and Amonton to determine the static friction coefficient from the experiments, the effect of memory in friction is not considered. Consequently, also in the numerical model this is not taken into account. In their work, Schulson and Fortt (2013) note that static strengthening can be detected only after a certain threshold value for the holding time and that this threshold period decreases with increasing velocity. At very low sliding velocities, the effect is clearly visible after 1 second, while the stick periods observed in our tests lasted up to maximum 0.13 seconds. Although the velocities in our tests are significantly higher, which may yield a decrease of the threshold period of 1 second, static strengthening was not observed during these tests. To be able to identify the static strengthening during stick-slip interaction, similar tests should be conducted at significantly lower sliding velocities.

Dry versus wet friction

In the analysis of the experimental data, as well as in the development of the numerical model, we have described the sliding interaction between the concrete and the ice by assuming dry friction. Especially at ambient temperatures near the freezing point, as well as due to frictional heating at the ice-concrete interface, the validity of this assumption may be questioned. It is commonly known that frictional heating may cause a small layer of ice to melt, thereby causing lubrication of the interface and a decrease of friction. According to Møen et al. 2015, this potentially explains the effect that a higher velocity yields a lower friction coefficient. Extensive melt and lubrication of the interface could prevent stick to occur from happening, thereby making the dry friction assumption invalid. During the experiments however, the ambient temperature was kept below the freezing point and, upon inspection after testing, no signs of ice surface melt were visible. As the friction coefficients used in the numerical model were derived from the test measurements, possible microscopic effects that have occurred during the test have also been taken into in the model. Therefore, it is concluded that the assumption of dry friction is valid.

Statistical comparison of the experimental data and the model results

To assess how well the numerical model matches the experiments performed, the output of the numerical model is compared to the complete set of experimental data. In order to statistically characterize the behavior of the ice sample on the rotating concrete slab, the mean and standard deviation of the ice sample displacement were determined for every experiment and thus for every data set from the test plan. Additionally, for every combination of the test variables, the same results were obtained from the numerical model. Note here that, due to the peaks observed in the experimental velocity curves, it was not possible to calculate the static friction coefficient for every combination of test variables given in Table 2, causing discrepancies in the displacement comparison.

Figure 9a shows the mean value and Figure 9b shows standard deviation of the ice sample displacement as obtained both experimentally and numerically for 39 different combinations of test variables. Figure 9 shows that for most tests, the mean displacements and standard deviations obtained experimentally and numerically match well. In general, it appears that the numerical model slightly underestimates both the mean and standard deviations obtained in the experiments. Nevertheless, the dependency on the test variables in the experimental tests and the numerical model
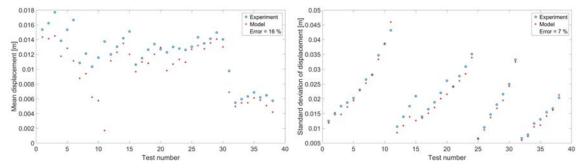

Figure 9: Comparison of test and model results: a) mean; b) standard deviation.

clearly have the same trends.

CONCLUSIONS

We have successfully designed an experimental set-up to investigate the stick-slip behavior of ice interacting with a concrete surface. The static friction coefficients observed have a range from 0.1 to 0.5, while the kinetic friction coefficient observed varies between 0.08 and 0.4. On average, the kinetic friction coefficient equals 0.7 times the static friction coefficient. The influence of varying sliding velocity, spring stiffness and normal load on the ice sample were investigated. While the mean of the friction coefficients shows a clear dependence, the influence on the standard deviation was limited. For the mean friction coefficients, the following trends were observed:

- μ_s decreases with an increase in normal load, m
- μ_k decreases with an increase in normal load, m
- μ_s slightly decreases with an increase in velocity, v
- μ_k decreases with an increase in velocity, v
- The influence of the spring stiffness was not identified, as the results of the analysis were contradicting.

Additionally, a model was developed and validated and it was shown that the numerical model statistically yields similar results as obtained during the measurement campaign. Table 3 below lists all the differences between the model and experiment

Table 3. Differences between the model and the experimental set-up.

Numerical Model	Experiment
1D behavior	2D behavior
Simulated randomness in friction coefficients	Natural randomness in friction coefficients
Constant μ_k during each period of slip	Time dependence of μ_k
No memory effect incorporated	Memory effect / static strengthening
Dry friction	Dry and possibly wet friction

REFERENCES

Bruneau, S.E., Dillenburg, A.K., Ritter, S. (2012). "Ice sample production techniques and indentation tests for laboratory experiments simulating ship collisions with ice". In: *International Society of Offshore and Polar Engineering.*

Fiorio, B., Meysonnier, J., Boulon, M. (2002). "Experimental study of the friction of ice over concrete under simplified ice-structure interaction conditions'. In: *Canadian Journal of Civil Engineering* 29, pp. 347-359.

Itoh, Y., Yoshida, A., Tsuchiya, M., Katoh, K., Sasaki, K., Saeki, H. (1988)."An experimental study on abrasion of concrete due to sea ice". In: *Offshore Technology Conference,* pp. 61-68.

ISO19906, 2010: Petroleum and natural gas industries – Arctic offshore structures.

Martins, J.A.C., J.T. Oden, F.M.F. Simoes (1990). "A study of static and kinetic friction". In: *International Journal of Engineering Science* 28, pp. 29-92.

Møen, E., Høiseth, K.V., Leira, B., Høyland, KV. (2015). "Experimental study of concrete abrasion due to ice friction – Part 1: Set-up, ice abrasion vs. material properties and exposure conditions". In: *Cold Regions Science and Technology* 110, pp. 183-201.

Terashima, T., Nakazawa, N. (1993). "Factors influencing the coefficient of friction between sea ice and various materials". In: *Port and Ocean Engineering Under Arctic Conditions,* pp. 97-105.

Saeki, H., Ono, T., Nakazawa, N., Sakai, M., Tanaka, S. (1986). "The coefficient of friction between sea ice and various materials used in offshore structures". In: *Journal of Energy Resources and Technology* 108, pp. 65-71.

Schulson, E.M., and Fortt, A.L. (2013). "Static strengthening of frictional surfaces of ice". In: *Acta Materialia* 61, pp. 1616-1623.

Tijsen, J.N.W. (2015). "Experimental study on the development of abrasion at offshore concrete structures in ice conditions". MA thesis. Delft University of Technology.